1. Artur BUGAŁA[1], 2. Antoni ARENDACZ[1], 3. Dorota BUGAŁA[1]

[1]Politechnika Poznańska, Instytut Elektrotechniki i Elektroniki Przemysłowej
ORCID: 1. 0000-0002-3321-4545; 3. 0000-0002-2579-448X

doi:10.15199/48.2024.02.17

Performance evaluation of bifacial photovoltaic module operating in standard and dedicated support structure

Streszczenie. *Niniejsza praca dotyczy analizy parametrów elektrycznych dwustronnego modułu fotowoltaicznego, wykonanego w technologii CELLO, przy jego instalowaniu w standardowej konstrukcji wsporczej, powszechnie wykorzystywanej w przypadku jednostronnych modułów fotowoltaicznych oraz przy zastosowaniu rozwiązania dedykowanego i pozbawionego elementów nośnych, mogących ograniczać dostęp odbitego promieniowania słonecznego do tylnej sekcji ogniw słonecznych. W pracy przedstawiono charakterystyki prądowo-napięciowe oraz mocy elektrycznej w pełnym zakresie obciążenia. Wykazano istotny wpływ rodzaju konstrukcji nośnej na wartość mocy elektrycznej osiąganej przy optymalnym obciążaniu a tym samym potrzebę weryfikacji aktualnych praktyk projektowych w zakresie stosowania modułów fotowoltaicznych dwustronnych zwłaszcza w przypadku powszechnych instalacji prosumenckich. (**Analiza wydajności dwustronnego modułu fotowoltaicznego pracującego w standardowej i dedykowanej konstrukcji wsporczej**).*

Abstract*. This paper concerns the analysis of electrical parameters of a double-sided photovoltaic module, made in the CELLO technology, when installed in a standard support structure, commonly used in the case of single-sided photovoltaic modules, and using a solution without supporting elements that may limit the access of reflected solar radiation to the rear side of solar cells. The paper presents current-voltage and power-voltage characteristics in the full load range. A significant impact of the type of supporting structure on the value of electric power achieved at optimal load was demonstrated, and thus the need to verify current design practices in the use of double-sided photovoltaic modules, especially in prosumer installations*

Słowa kluczowe: moduł dwustronny, technologia CELLO, zysk energetyczny, konstrukcja montażowa.
Keywords: double-sided module, CELLO technology, energy gain, assembly structure.

Introduction

In recent years, a significant increase in interest in modern and non-standard solutions in the field of photovoltaic installations is visible, such as Sun tracking systems [1], solar radiation concentrators, multi-colored photovoltaic modules, modules with unusual shapes [2] or double-sided solar cells. Many of these solutions were conceptualized decades ago.

The technology of double-sided photovoltaic modules was developed in the 1960s. Bifacial photovoltaics is currently a rapidly growing technology that can improve electricity production by utilizing solar radiation from both sides (the front and the rear) of the photovoltaic module [3]. Monofacial cells can only collect photons reaching the front side of the solar photo converter.

The rear part of the bifacial modules is, in most cases, built similarly to the front part, and the structure of the active semiconductor layer is covered with glass. There are solutions like glass-glass bifacial modules, where the module is completely devoid of a typical structural frame [4], as well as solutions equipped with a narrower and lower aluminum profile. In both cases, the PV module is not equipped with a classic plastic substrate, which translates into decrease in solar cells working temperature and increase in maximum power output due to the reduced infrared absorption.

Figure 1 shows a cross-section of the standard bifacial crystalline silicon solar cells.

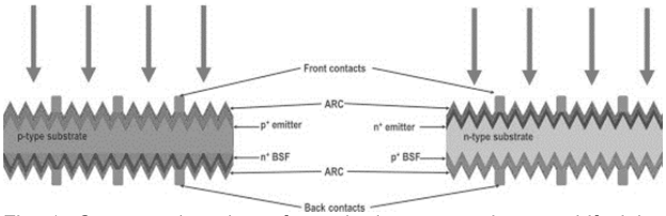

Fig. 1. Cross-section view of standard n-type and p-type bifacial crystalline silicon solar cell [5]

Currently, many technologies can be distinguished among double-sided solar cells [6]:

- passivated emitter rear contact PERC,
- passivated emitter rear locally-diffused PERL,
- passivated emitter rear totally difused PERT,
- heterojunction with intrinsic thin-layer HIT,
- integrated back contact IBC,
- double-sided buried contact solar cel DSBCSC.

Double-sided photovoltaic modules are described by operational parameters such as bifaciality factor *BF*, separation factor *SR*, bifacial energy gain *BGE* and irradiation *g*.

Factors affecting the energy efficiency of bifacial PV modules include the angle of their inclination to the ground, mounting height above ground level, the value of the ground albedo coefficient, the share of diffuse radiation in the global radiation spectrum or the type of mounting system.

There are numerous mounting systems solutions for single-sided and double-sided photovoltaic modules, such as roof structures, ground structures, intended for agrophotovoltaics or carport systems [7]. Among the mounting structures, there are systems dedicated to use specifically with double-sided modules. In standard designs, the transverse support elements run directly under the surface of the modules, which can be a source of shading of the cells located in the rear part and contribute to reducing the radiation reflected from the ground surface. Described problem does not occur with single-sided modules. Therefore, constructions in which horizontal and vertical supporting crossbars will be located outside the surface of photovoltaic cells are gaining importance.

Solar radiation distribution in the case of bifacial photovoltaic module

Total solar radiation I_{tot} recorded in the plane of the bifacial PV module is the sum of the direct radiation I_{beam}, diffused radiation I_{diff}, and reflected radiation I_{alb} from the ground located under the module. The components of solar radiation are presented in figure 2. The total irradiance is described by the relation [8][9]:

(1) $$I_{tot} = I_{beam} + I_{diff} + I_{alb}$$

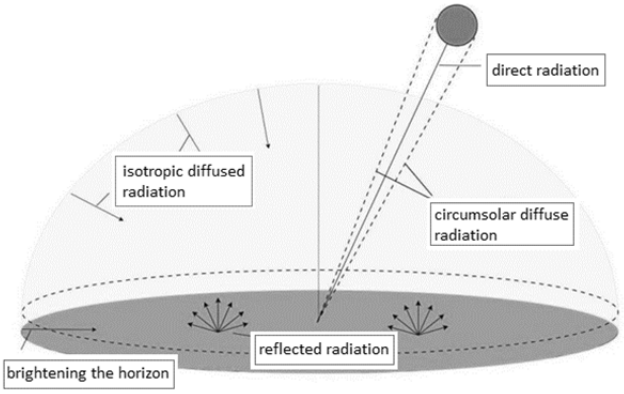

Fig.2. Components of solar radiation [8]

The orientation of the photovoltaic module and the position of the Sun can be described by appropriate angles presented in figure 3. The position of the Sun consists of the azimuth angle γ_S and the angle of the Sun's elevation above the horizon α_S The irradiance recorded on the surface of the module depends on the angle of its azimuth γ and inclination β.

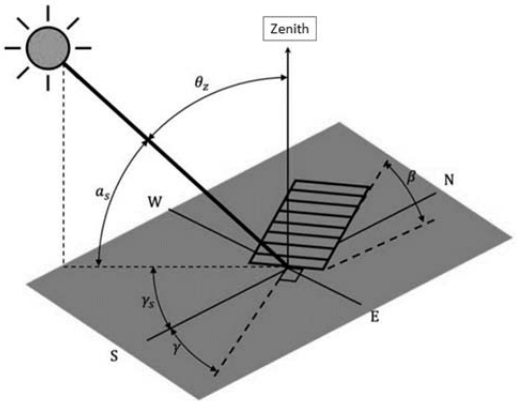

Fig.3. Angles describing the position of the module and the Sun

The angle of incidence of solar radiation on the surface of the module is the angle between the radiation beam and the normal to this surface. The angle of incidence on the front or rear side of the module is described by the relation [10]:

(2) $\theta_{F/R} = \cos\theta_z \cdot \cos\beta_{F/R} + \sin\beta_{F/R} \cdot \sin\theta_z \cdot \cos(\gamma_s - \gamma_{F/R})$

where: $\theta_{F/R}$ - angle of incidence of radiation for the front or rear side of the module, $\beta_{F/R}$ - angle of inclination for the front or rear side of the module, $\gamma_{F/R}$ - azimuth angle for the front or rear side of the module.

The additional energy gain in the case of using a double-sided photovoltaic module is the result of the size of the share of radiation reflected in the global spectrum of solar radiation.

In case of modeling of solar radiation, the greatest difficulty is the accurate estimation of the diffused radiation recorded on the plane of the tilted PV module. There are isotropic, pseudoisotropic and anisotropic mathematical models available in the literature [11]. One of the most accurate is the Perez anisotropic solar radiation model. The model divides the diffused radiation into three components: isotropic radiation, circumsolar radiation focused around the Sun and horizontal scattered radiation centered around the horizon line. The components of the diffused radiation on the inclined surface of the PV module can be represented by the relationship [12]:

(3) $I_{diff,iso,F/R} = I_{DHI} \cdot (1 - F_1) \cdot \left(\frac{1+\cos\beta_{F/R}}{2}\right) \cdot \left(1 - R_{loss,iso}^{F/R}\right)$

(4) $I_{diff,cir,F/R} = I_{DHI} \cdot F_1 \cdot \frac{a_{F/R}}{b} \cdot \left(1 - R_{loss,cir}^{F/R}\right)$

(5) $I_{diff,hor,F/R} = I_{DHI} \cdot F_2 \cdot \sin\beta_{F/R} \cdot \left(1 - R_{loss,iso}^{F/R}\right)$

where: F_1 - coefficient of circumsolar brightness, F_2 - coefficient of brightness of the horizon, $a_{F/R}$ and b - coefficients taking into account the angle of incidence of circumsolar radiation.

The coefficients F_1 and F_2 can be determined using the relations [12]:

(6) $$F_1 = f_{11} + f_{12} \cdot \Delta + \frac{\pi \cdot \theta_z}{180} \cdot f_{13}$$

(7) $$F_2 = f_{21} + f_{22} \cdot \Delta + \frac{\pi \cdot \theta_z}{180} \cdot f_{23}$$

where: f_{11}, f_{12}…f_{23} – brightness coefficients depending on the purity of the sky and the angle zenith, Δ – brightness parameter.

The purity of the sky ε and the brightness parameter Δ are also determined by the Perez model [12]:

(8) $$\varepsilon = \frac{\left(\frac{I_{DHI}+I_{DNI}}{I_{DHI}}\right)+1.041\cdot\left(\frac{\pi\cdot\theta_z}{180}\right)^3}{1.041\cdot\left(\frac{\pi\cdot\theta_z}{180}\right)^3}$$

(9) $$\Delta = \frac{I_{DHI}\cdot m}{I_{EXTRA}}$$

where: m – air mass, I_{EXTRA} – extraterrestrial radiation.

Table 2. Brightness coefficients depending on the sky purity parameter [13]

ε	f_{11}	f_{12}	f_{13}	f_{21}	f_{22}	f_{23}
1,000 - 1,065	-0,008	0,588	-0,062	-0,06	0,072	-0,022
1,065 - 1,230	0,13	0,683	-0,151	-0,019	0,066	-0,029
1,230 - 1,500	0,33	0,487	-0,221	0,055	-0,064	-0,026
1,500 - 1,950	0,568	0,187	-0,295	0,109	-0,152	-0,014
1,950 - 2,800	0,873	-0,392	-0,362	0,226	-0,462	0,001
2,800 - 4,500	1,132	-1,237	-0,412	0,288	-0,823	0,056
4,500 - 6,200	1,060	-1,600	-0,359	0,264	-1,127	0,131
6,200 - ∞	0,678	-0,327	-0,250	0,156	-1,377	0,251

Radiation reflected from the ground surface

The intensity of radiation reflected from the ground, which can contribute to the generation of electricity in a bifacial module, can be divided into three components [14]:

(10) $I_{alb,F/R} = \left(I_{alb,F/R}^{beam} + I_{alb,F/R}^{diff,iso} + I_{alb,F/R}^{diff,cir}\right) \cdot \left(1 - R_{loss,alb}^{F/R}\right)$

where: $I_{alb,F/R}$ – total intensity of reflected radiation, $I_{alb,F/R}^{beam}$ – component of reflected radiation resulting from the intensity of direct radiation, $I_{alb,F/R}^{diff,iso}$ – component of reflected radiation resulting from the isotropic part of the diffuse radiation, $I_{alb,F/R}^{diff,cir}$ – component of reflected radiation resulting from circumsolar diffuse radiation, $R_{loss,alb}^{F/R}$ – reflection losses the front and back of the module for radiation reflected from the surface of the substrate.

Only part of the radiation is reflected from the earth's surface and has a chance to be converted into electricity. This is due to the shading effect generated by photovoltaic modules. In order to determine the share of reflected radiation in the generation of electric power by bifacial module, the values of the view factors of the surface are determined [15].

Losses related to the reflection of solar radiation

When performing irradiance calculations for both sides of a bifacial module, it is important to take into account the angular losses associated with reflection from the surface of the module. Reflection losses depend on the angle of incidence of radiation on its surface. The size of the losses can be described by the relationships [16][17]:

$$R_{loss,beam}^{F/R} = \frac{\exp\left(\frac{-\cos\theta_{F/R}}{a_r}\right) - \exp\left(\frac{-1}{a_r}\right)}{1-\exp\left(\frac{-1}{a_r}\right)} \tag{11}$$

$$R_{loss,hor}^{F/R} = \frac{\exp\left(\frac{-\cos\theta_{hor,F/R}}{a_r}\right) - \exp\left(\frac{-1}{a_r}\right)}{1-\exp\left(\frac{-1}{a_r}\right)} \tag{12}$$

$$R_{loss,alb}^{F/R} = \exp\left[-\frac{1}{a_r}\left(c_1 \cdot \left(\sin\beta + \frac{\left(\frac{\pi\cdot\beta}{180}\right) - \sin\beta}{1-\cos\beta}\right) + c_2 \cdot \left(\sin\beta_{F/R} + \frac{\left(\frac{\pi\cdot\beta}{180}\right) - \sin\beta}{1-\cos\beta}\right)\right)\right] \tag{13}$$

$$R_{loss,iso}^{F/R} = \exp\left[-\frac{1}{a_r}\left(c_1 \cdot \left(\sin\beta_{F/R} + \frac{\left(\frac{\pi\cdot\beta}{180}\right) - \sin\beta_{F/R}}{1-\cos\beta_{F/R}}\right) + c_2 \cdot \left(\sin\beta_{F/R} + \frac{\left(\frac{\pi\cdot\beta}{180}\right) - \sin\beta_{F/R}}{1-\cos\beta_{F/R}}\right)\right)\right] \tag{14}$$

where: $R_{loss,beam}^{F/R}$ – reflection losses of the front and rear of the module for direct radiation, $R_{loss,hor}^{F/R}$ – reflection losses of the front and rear of the module for horizontal diffuse radiation, $R_{loss,alb}^{F/R}$ – reflection losses of the front and rear of the module for radiation reflected from the surface of the substrate, $R_{loss,iso}^{F/R}$ – reflection losses of the front and rear of the module for isotropic scattered radiation, a_r – angular loss coefficient, c_1 and c_2 – matching parameters.

The values of the angular loss coefficient and matching parameters depend on the construction of the module. These are values determined empirically. Technologies used and materials as well as dirt affect the behavior of light reaching the surface of the module. Table 1 shows the values of a_r for various PV module technologies [16-19].

Table 1. Angular loss factor for different PV cell technologies

Photovoltaic cell technology	Coefficient a_r
crystalline silicon	0,21
amorphous silicon	0,23
heterojunction cells	0,22
cadmium-tellurium cells	0,23
indium-copper cells	0,20

Measurement and research stand

A laboratory test stand was designed and built to enable the determination of the electrical parameters of a bifacial PV module with the possibility of installing additional (horizontal and vertical) elements in the construction of the mounting system and their elimination, in order to indicate the differences between the standard supporting structure and the structure dedicated for bifacial photovoltaic modules. Laboratory conditions allow to maintain a constant value of irradiance during measurements. Designed solution allows to adjust the angle of inclination of the PV module (15º, 30˚ or 45˚), modify the position of the module above ground level and install a photovoltaic module of any geometric dimensions.

The measurement and research stand consists of the tested double-sided photovoltaic module LG Neon 2 Bifacial LG390N2T-A5, a system for recording current and voltage, a set of adjustable resistors, and HT204 pyranometer. The light source is a mobile system of 12 halogen lamps divided into 3 sections (upper, middle and lower lines, 4 pieces each). The photovoltaic module consists of 72 N-type monocrystalline silicon cells. It was made in CELLO technology (Cell Connection, Electrically, Low Loss, Low Stress, Optical Absorbtion Enhancement). The technology is characterized by the reduction of current losses and allows to improve the absorption of radiation by solar cells. Current losses are limited by the use of 12 microfibers for each solar cell (as opposed to 3 flat wires in classic one-sided cells). Figure 4 shows the prepared test stand with the measuring unit.

Fig. 4. Test stand in one of the configurations, module mounting height 120 cm, inclination angle 30º.

Figure 5 shows two selected variants with additional structural elements for the mounting system (steel profiles perpendicular and parallel to the photovoltaic cells), in order to determine the impact of their presence on the electrical parameters of the tested bifacial photovoltaic module. In the case of a mounting systems dedicated to bifacial modules, additional profiles do not exist or are designed in places that do not coincide with solar cells located in the back side of the photovoltaic module.

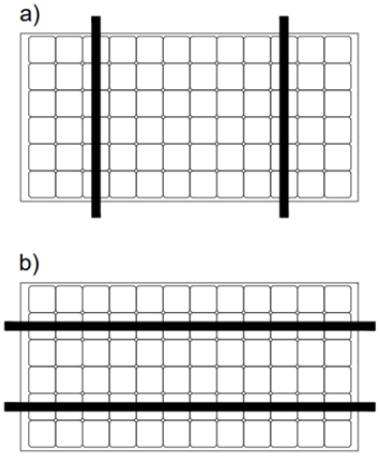

Fig. 5. Arrangement of additional elements of the supporting structure for a bifacial photovoltaic module, a) perpendicular profiles, b) parallel profiles

Results

The tests were carried out for three different ground types: PVC material, polyester material and a white laminated

wooden board placed under the PV module. For each of the substrates, the albedo coefficient was determined (0.43, 0.59 and 0.67, respectively).
The photovoltaic module was illuminated using two rows of light sources, achieving an average irradiance of 125 W/m^2 on its front surface. The module was placed at a height of 120 cm. The angle of inclination of the module to the ground was equal to 30º. The distance between the light source and the frame of the photovoltaic module was 80 cm. Figures 6, 8 and 10 show the current-voltage characteristics of the photovoltaic module, while figures 7, 9 and 11 show the power-voltage characteristics.

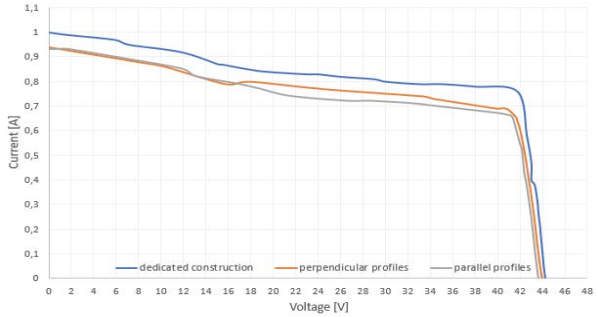

Fig. 6. Current-voltage characteristics of a double-sided photovoltaic module for a substrate in the form of laminated wooden board

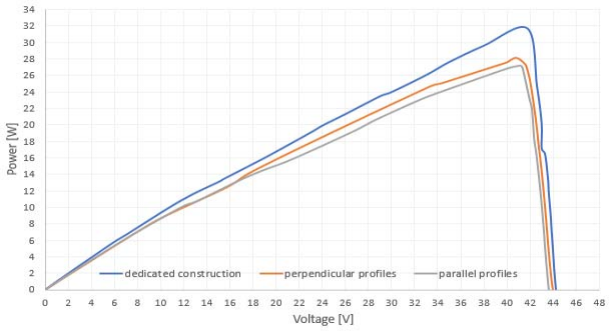

Fig. 7. Power-voltage characteristics of a double-sided photovoltaic module for a substrate in the form of laminated wooden board

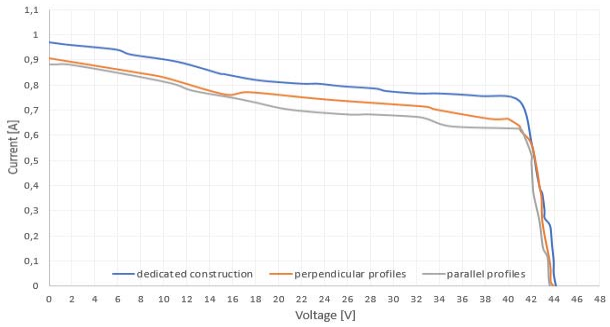

Fig. 8. Current-voltage characteristics of a double-sided photovoltaic module for a substrate in the form of polyester material

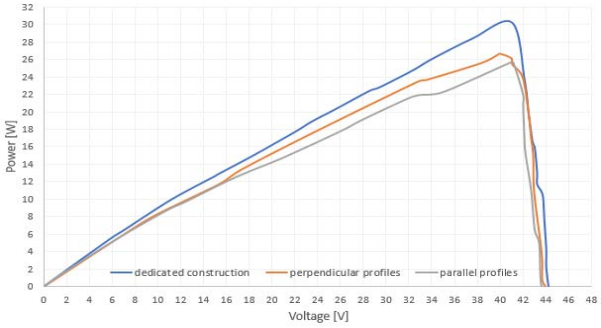

Fig. 9. Power-voltage characteristics of a double-sided photovoltaic module for a substrate in the form of polyester material

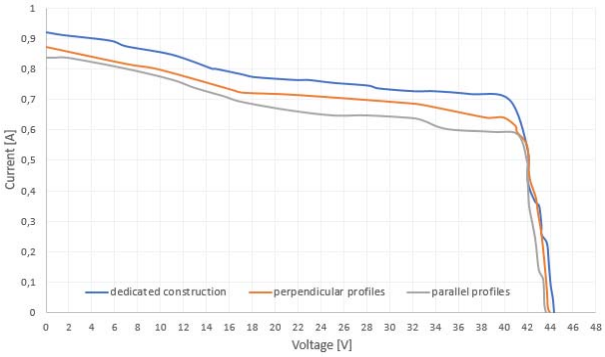

Fig. 10. Current-voltage characteristics of a double-sided photovoltaic module for a substrate in the form of PVC material

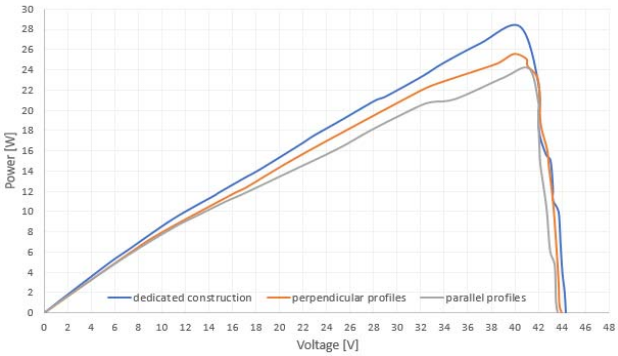

Fig. 11. Power-voltage characteristics of a double-sided photovoltaic module for a substrate in the form of PVC material

Conclusions

Estimation of electric energy production using bifacial photovoltaic modules is more complicated than for classic one-sided modules. When connecting bifacial modules series or parallel, it is important to ensure identical environmental conditions in order to reduce the risk of current or voltage mismatch between individual generators.
An important factor affecting the energy efficiency of a double-sided module is the use of an appropriate mounting solution. There are mounting structures, characterized by the presence of profile elements that can provide a source of shading for the cells located in the rear side of the bifacial PV module. Manufacturers of photovoltaic mounting solutions, dedicated to bifacial modules, do not inform about their actual impact on the operation of the photovoltaic installation. There is also a limited choice of mounting structures for bifacial PV modules, and this problem is particularly visible in the case of glass-glass bifacial modules.
Based on the conducted research, it can be concluded that the use of a properly designed mounting structures can bring greater benefits to cases characterized by a higher albedo coefficient of the ground under the photovoltaic module.
The mounting structure with parallel profiles (fig. 5b) was characterized in each case by a higher power loss (compared to the reference solution without parallel and perpendicular profiles) than the one resulting from the use of perpendicular crossbars. Parallel placement of the profiles, relative to the longer edge of the PV module, leads to an increase in the area covered by the shadow.
Based on the measurements, for the surface under the module with the highest reflectivity and for the absence of any structural profiles in the back side of the PV module, the maximum power of 31.7 W was obtained. The use of additional perpendicular and parallel load-bearing profiles

leads to a reduction of electric power by 11.3% and 14.6%, respectively.

Changing the type of substrate and the use of polyester material leads to the achievement of electric power at the optimal load equal to 30.2 W. The use of additional perpendicular and parallel bearing profiles leads to a reduction of electric power by 10.8% and 14.1%, respectively. In the case of the substrate with the lowest value of the reflectivity coefficient, the maximum power of 28.2 W was obtained, without the use of additional structural profiles. The use of additional perpendicular and parallel supporting profiles leads to a reduction of electric power by 9.6% and 12.7%, respectively.

The higher the reflectivity of the substrate under the double-sided PV module, the more significant the impact of additional mounting system structural elements.

A reduction in a short-circuit current was observed when the module was installed above the substrate described by low reflectivity. However, the open-circuit voltage does not change significantly.

It can also be assumed that the specific construction of bifacial photovoltaic modules, with their appropriate connection in a photovoltaic installation with single-sided modules, enables the shaping and better matching of the energy production profile and the demand profile.

The analysis of a photovoltaic installation operation composed of double-sided and single-sided PV modules will be the subject of further research.

***Autorzy**: dr inż. Artur Bugała, Politechnika Poznańska, Instytut Elektrotechniki i Elektroniki Przemysłowej, ul. Piotrowo 3a, 60-965 Poznań, E-mail: artur.bugala@put.poznan.pl; dr inż. Dorota Bugała, Politechnika Poznańska, Instytut Elektrotechniki i Elektroniki Przemysłowej, ul. Piotrowo 3a, 60-965 Poznań, E-mail: dorota.bugala@put.poznan.pl; mgr inż. Antoni Arendacz, Politechnika Poznańska, Instytut Elektrotechniki i Elektroniki Przemysłowej, ul. Piotrowo 3a, 60-965 Poznań, E-mail: antoni.arendacz@zenerisprojekty.pl*

REFERENCES

[1] Sawicka-Chudy P., Cholewa M., Sibiński M., Pawełek R., Analiza parametrów modułów fotowoltaicznych stacjonarnych i nadążnych w warunkach rzeczywistych, *Przegląd Elektrotechniczny*, 92, 9 (2016), 58-61

[2] Pawlak R., Kawczyński R., Korzeniewska E., Lebioda M., Rosowski A., Rymaszewski J., Sibiński M., Tomczyk M., Walczak M., Ogniwa fotowoltaiczne o niekonwencjonalnych kształtach, *Przegląd Elektrotechniczny*, 89, 7 (2013), 288-292

[3] Kopecek R., Bifacial Photovoltaics 2021: Status, Opportunities and Challenges, *Energies*, 14 (2021), 2076, https://doi.org/10.3390/en14082076

[4] Qingzhu W., Chenyang W., Xiaorui L., Sanyang Z., Feng Q., Junyu L., Weifei L., Paul N., The Glass-glass Module Using n-type Bifacial Solar Cell with PERT Structure and its Performance, *Energy Procedia*, 92 (2016), 750-754, https://doi.org/10.1016/j.egypro.2016.07.054

[5] Guerrero-Lemus R., Vega R., Taehyeon K., Kimm A., Shephard L.E., Bifacial solar photovoltaics – A technology review, *Renewable and Sustainable Energy Reviews*, 60 (2016), 1533-1549, https://doi.org/10.1016/j.rser.2016.03.041

[6] Liang T. S., Pravettoni M., Deline Ch., Stein J., A review of crystalline silicon bifacial photovoltaic performance characterization and simulation, *Energy & Environmental Science,* 1 (2019), https://doi.org/10.1039/C8EE02184H

[7] Arabach J.R., Schneider A., Mrcarica M., Kopecek R., Heckmann M., The Need of Frameless Mounting Structures for Vertical Mounting of Bifacial PV Modules, 32nd European Photovoltaic Solar Energy Conference and Exhibition, München, Germany, 2016, https://doi.org/10.4229/EUPVSEC20162016-5CO.14.5

[8] Nygren A., Sundstrom E., Modelling Bifacial Photovoltaic Systems, Evaluating the albedo impact on bifacial PV systems based on case studies in Denver, USA and Västerås, Sweden, *Mälardalen University, Sweden, 2021, diva-portal.org*

[9] Chaouki G., Fahad F. A., Oussama R., Abdul K. H., Sensitivity analysis of design parameters and power gain correlations of bi-facial solar PV system using response surface methodology, *Solar Energy*, 223 (2021), 44-53, https://doi.org/10.1016/j.solener.2021.05.024

[10] Duffie J. A., Beckman W. A, Solar Engineering of Thermal Processes, Solar Energy Laboratory, University of Wisconsin-Madison, 2013

[11] Frydrychowicz–Jastrzębska G., Bugała A., Modeling the distribution of solar radiation on a two–axis tracking plane for photovoltaic conversion, *Energies*, 8, 2 (2015), 1025–1041, https://doi.org/10.3390/en8021025

[12] Perez R., The development and verification of the Perez diffuse radiation model, Report, Atmospheric Sciences Research Center, Albany NY, USA, 1988

[13] Perez R., Modeling daylight availability and irradiance components from direct global irradiance, Report, Atmospheric Sciences Research Center, Albany NY, USA, 1990

[14] Sun X., Khan M. R., Deline Ch., Alam M. A., Optimization and performance of bifacial solar modules: A global perspective, *Applied Energy*, 212 (2018), 1601-1610, https://doi.org/10.1016/j.apenergy.2017.12.041

[15] Appelbaum J., The role of view factors in solar photovoltaic fields, *Renewable and Sustainable Energy Reviews*, 81 (2018), 161-171, https://doi.org/10.1016/j.rser.2017.07.026

[16] Martin N., Ruiz J. M., A new model for PV modules angular loses under field conditions, *International Journal of Solar Energy*, 22 (2002), 19-31, https://doi.org/10.1080/01425910212852

[17] Martin N., Ruiz J. M., Annual Angular Reflection Losses in PV Modules, *Progress in photovoltaics: Research and Applications*, 13 (2005), 75-84, https://doi.org/10.1002/pip.585

[18] Zarei T., Abdolzadeh M., Soltani M., Aghanajafi C., Computational investigation of dust settlement effect on power generation of three solar tracking photovoltaic modules using a modified angular losses coefficient, *Solar Energy*, 222 (2021), 269-289, https://doi.org/10.1016/j.solener.2021.04.059

[19] Chivelet M., Chenlo F., Mejuto E., Validating an angular of incidence losses model with different PV technologies and soiling conditions, 26th european Photovoltaic Solar Energy Conference, Frankfurt, 2012